Energy-based model of a solar-powered pumped-hydro storage system

Phillips Brenes, Hayden; Pereira Arroyo, Roberto; Muñoz Arias, Mauricio

Energy-based model of a solar-powered pumped-hydro storage system

Hayden Phillips-Brenes
School of Electronics Engineering
Costa Rica Institute of Technology
Alajuela, Costa Rica
hphillips@itcr.ac.cr

Roberto Pereira-Arroyo
School of Electronics Engineering
Costa Rica Institute of Technology
Alajuela, Costa Rica
rpereira@itcr.ac.cr

Mauricio Muñoz-Arias
Faculty of Science and Engineering
University of Groningen
Groningen, The Netherlands
m.munoz.arias@rug.nl

***Abstract*—This document presents a port-Hamiltonian model of a pumped-hydro storage system, using Photo Voltaic energy as the primary source. Matlab simulation results show that the model is functional under ideal conditions of constant solar radiation. It also graphically demonstrate the relationship between input solar power and the accumulation of energy at the upper reservoir.**

This work is a fundamental step towards a tool for the analysis and design of optimized and fully automated system.

***Index Terms*—energy storage, pumped-hydro system, photo-voltaic energy, port-Hamiltonian systems.**

I. Introduction

During the last four years (2015-2018), more than 98% of Costa Rica's electricity came from green sources, mainly produced by hydroelectric power [1]. However, during the dry season, the lack of rain makes it necessary to use fossil fuel generating plants to cover the energy deficit during peak hours.

Although the deficit is relatively a small amount of energy (1.88%) compared to the total electrical energy consumed by the country, it has a much higher cost per kWh which is transferred to the costumers. Also, consume of non-green energy sources produces carbon dioxide emissions, which goes against the goals of decarbonizing the Costa Rican economy [2].

It is possible to employ solar radiation as an alternative energy source. During the dry season, solar radiation in Costa Rica reaches the highest level, with several zones receiving a daily average of $5kWh/m^2$ [3]. This represent a huge potential which has not been exploited as only 0.01% of the electricity is generated with the solar resource. However, the intermittent characteristic of photo-voltaic power generation is a drawback to increase its penetration in the country.

This paper describes the use of solar radiation energy to power an pumped-hydro system, as a way to foster the widespread in a large-scale of green sources systems is investigated.

By employing this class of storage system, the energy generated by the alternative sources systems can be accumulated as potential energy of water and then released at a higher power rate, when the peak demand is not met by the national electric grids renewable installed capacity. This would avoid the use of fossil fuels in thermal back up plants.

978-1-7281-0883-4/19/$31.00 ©2019 IEEE

Pumped-hydro storage (PHS) is the most widespread energy storage technology, which has been in use for more than a hundred years and has a round trip efficiency of 70 to 85% [4]. It is also the most cost-effective for large scale energy storage in utility grids. In the PHS, the work of [5] and [6] is recapitulated. The concept of the proposed system is shown in Figure 1.

We based our work firstly on the results of [5] by using solar radiation and rewriting the system on an energy-based setting, more specifically on the port-Hamiltonian framework due to the straightforward interpretation of the physical interconnection of multiple systems domains via power-ports, and energy dissipating and storing elements, [7]–[9]. Then, the main result of this paper is a port-Hamiltonian representation of a solar-pumped energy storage system where we clearly show how the internal energy of the system flows in different physical domains which in later research developments will facilitate the integration of other systems' stages and the design of (non)linear controllers.

The contribution of the paper is outlined as follows. Section II presents an general introduction to the port-Hamiltonian formalism. Furthermore, Section III provides the energy-based model of the proposed solar-powered pumped-hydro storage system. Later on, we reinforced the modeling advantages with simulation results in Section IV. Finally, in Section V concluding remarks and future work are provided.

Notation: The Gradient of a scalar vector is given by

$$\nabla_x := \frac{\delta}{\delta x}. \tag{1}$$

Furthermore, all vectors are considered as column vectors.

II. port-Hamiltonian framework

In this section, we present the port-Hamiltonian (PH) formalism for a general class of physical systems, and later we present a formulation for a standard class of mechanical systems.

The PH framework is based on the description of systems in terms of energy variables, their interconnection structure, and power port-pairs. PH systems include a large family of physical nonlinear systems which includes the dynamics of mechanical, electrical, hydraulic, and electromechanical subsystems. The transfer of energy between the physical system and the environment is given through energy elements, dissipation elements and power preserving ports, [7]–[9].

A time-invariant PH system corresponds to the

$$\Sigma \begin{cases} \dot{x} = \left[\mathcal{J}\left(x\right) - \mathcal{R}\left(x\right)\right] \nabla_x H\left(x\right) + g\left(x\right) u, \\ y = g\left(x\right)^\top \nabla_x H\left(x\right), \end{cases} \tag{2}$$

where the state variable is given by $x \in \mathcal{R}^{\mathcal{N}}$, and the input-output port-pair representing flows and efforts are given by

$$u \in \mathcal{R}^{\mathcal{N}}, \tag{3}$$

$$y \in \mathcal{R}^{\mathcal{M}}, \tag{4}$$

respectively. Furthermore, the input, interconnection and dissipation matrices of (2) are given by

$$g\left(x\right) \in \mathcal{R}^{\mathcal{N}\times\mathcal{M}}, \tag{5}$$

$$\mathcal{J}\left(x\right) = -\mathcal{J}\left(x\right)^\top, \; \mathcal{J}\left(x\right) \in \mathbb{R}^{\mathcal{N}\times\mathcal{N}}, \tag{6}$$

$$\mathcal{R}\left(x\right) = \mathcal{R}\left(x\right)^\top \succeq 0, \; \mathcal{R}\left(x\right) \in \mathbb{R}^{\mathcal{N}\times\mathcal{N}}, \tag{7}$$

where $\mathcal{M} \leq \mathcal{N}$ being $\mathcal{M} = \mathcal{N}$ a fully actuated system, and $\mathcal{M} < \mathcal{N}$ an underactuated one. Furthermore, the energy function of system (2) is

$$H\left(x\right) \in \mathbb{R}. \tag{8}$$

Differentiating the Hamiltonian along the trajectories of $\dot{x}$, we recover the energy balance

$$\dot{H}\left(x\right) = -\nabla_x^\top H\left(x\right) \mathcal{R}\left(x\right) \nabla_x H\left(x\right) + y^\top u \leq y^\top u \tag{9}$$

where we clearly see how the system (2) is conservative.

III. Energy-based model of the system components

The system under study consists of different stages that are able to convert solar radiation in hydro potential energy. First, a *photovoltaic cell farm* works as a source of energy. The output of the first stage is manipulated by a *dc-dc buck converter* in order to feed an electromechanical *pumped-hydro stage*. It follows that the pump system is able to elevate a column of water via a *water recovery pipe* from a lower to an *upper reservoir*. The complete system is shown in Figure 1 with a more detailed block diagram given by Figure 2, where the inputs and outputs of each of the subsystems (domains) are presented. We see in Figure 2 how the system has as input the current i_s that depends on the radiation of the sun G, and as output the hydraulic flow Q_c.

Table I shows all parameters used through the modeling of the system stages.

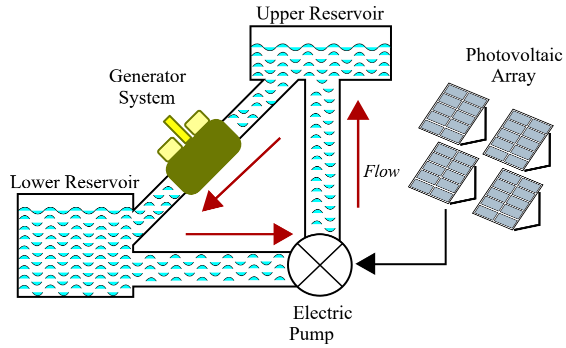

Fig. 1. Concept of the solar-powered pumped-hydro system for energy storage.

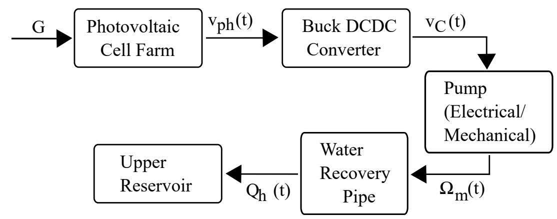

Fig. 2. Block diagram of the energy storage system's domains.

A. Photovoltaic Farm Model

A photovoltaic (PV) cell has the same behavior as a diode, connected to a parallel capacitor, and to parallel and serial resistors. The PV cell generates electricity when irradiated by light. One of the most complete expressions to model the electrical behavior of PV modules is the *five-parameter model* of [14]. It can be included also the parallel capacitance of the semiconductors, that has been previously calculated by [15]. The equivalent circuit of the PV cell of [16] is shown in Figure 3.

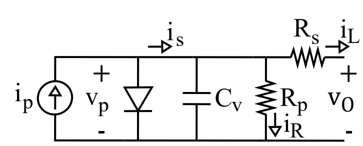

Fig. 3. Photovoltaic cell equivalent circuit.

The input-output port-pair of the PV cell module is given by (v_p, i_L), respectively. The current i_L at the output of the PV cell farm module depends on the S time function of the switch at the input of the dc/dc buck converter module that we introduce later on. Then, by Kirchhoff's current law for the PV cell farm equivalent circuit it follows that

$$i_C = -i_R + i_s - S i_L, \tag{10}$$

where

$$i_s = i_p - I_D, \tag{11}$$

and

$$i_p = N_p i_p, \tag{12}$$

TABLE I
PARAMETERS FOR PORT-HAMILTONIAN SYSTEM MODELING

Constant /Variable	Description		
	Detail	***Value***	***Units***
i_p	Photo generated current	N/A	A
k	Boltzmann constant	$1.38x10^{-23}$	J/K
T	Enviroment temperature	25	°C
q	Charge of electron	$1.62x10^{-19}$	C
$V_t = \frac{kT}{q}$	Thermal voltage p-n diode	25	mV
V_g	Band gap of Silicium	$1.76x10^{-19}$	J
T_v	PV Cell temperature	30	°C
r_s	In-PV series resistor[a]	6.81	Ω
r_p	In-PV parallel resistor[a]	13.2	Ω
n	pn junction ideality factor	1	N/A
i_0	pn diode saturation current	N/A	A
N_s	Number of series cells	1	N/A
N_p	Number of parallel cells	2	N/A
c_v	PV Cell capacitance	2.5	μF
$I_{SC,nom}$	Short circuit current[b]	7.6	A
$V_{OC,nom}$	Open circuit voltage[b]	32.8	V
G_{Sun}	Sun Radiation	N/A	kW/m^2
G_{nom}	PV onminal Radiation	1000	kW/m^2
K_0	I_{SC}/T_v coefficient of PV	2.3	mA/K
C_c	Converter capacitance[c]	8	mF
L_c	Converter inductance[c]	300	mH
S	Square function period[c]	20	ms
L_m	Armature inductance[d]	1.42	mH
R_m	Armature resistance[d]	1.3	$m\Omega$
J_m	Rotor inertia[d]	38.3	mg/m^2
B_m	Rotor friction[d]	34.7	μNms
K_m	Torque constant[d]	0.059	Nm/A
K_e	Voltage constant[d]	0.059	V/s
C_h	Hydraulic capacitance[e]	2.6	$g/(ms)^4$
I_h	Hydraulic inertance[f]	$2.03x10^7$	kg/m^4
R_h	Hydraulic resistance[g]	$9.28x10^5$	$kg/(m^4s)$
K_h	Speed-flow constant[h]	$1.91x10^5$	rad/m^3
ρ	Water density	998.2	kg/m^3
g	Gravity constant	9.81	m/s^2
μ	Water viscosity	890	$\mu Nm/s^2$
l	Pipe length	10	m
d	Pipe diameter	25	mm
Ω_{nom}	Nominal angular speed[d]	55	rev/s
Q_{nom}	Nominal flow[i]	$1.81x10^{-3}$	m^3/s

[a] Previously calculated by [10] for $175W$ PV.
[b] Measured at G_{nom}, from PV data sheet [11].
[c] Adjusted to ensure $24V$ at dc-dc converter output at G_{nom} [11].
[d] Motor P/N:211333, from data sheet [12].
[e] $C_h = A_R/(\rho g)$, A_R the reservoir area of $25m^2$.
[f] $I_h = \rho l/A_p$, with A_p the area of pipe cross section.
[g] $R_h = 8\pi\mu l/A_p^2$, from Poiseuille law.
[h] $K_h = 2\pi\Omega_{nom}/Q_{nom}$.
[i] Water Pump P/N:RD9024, from data sheet [13].

$$I_D = N_p i_0 \left(\exp\left(\frac{V + i_L \dfrac{N_s}{N_p} r_s}{N_s n V_t} \right) - 1 \right) = N_p i_0 \left(\exp\left(\frac{v_p}{N_s n V_t} \right) - 1 \right). \tag{13}$$

In (13), a current accross the diode is represented by I_D. Furthermore, according to [17] the currents i_p of (12), and i_0 in (13) are defined as

$$i_p = (I_{SC,nom} + K_0 (T - T_v)) \frac{G_{Sun}}{G_{nom}}, \tag{14}$$

$$i_0 = i_\alpha \left(\frac{T}{T_v}\right)^{\frac{3}{n}} \exp\left(\frac{-V_g}{nk} \left(\frac{1}{T} - \frac{1}{T_{pv}} \right) \right), \tag{15}$$

respectively, with i_α in (15) given by

$$i_\alpha = \frac{I_{SC,nom}}{\exp\left(\dfrac{V_{OC,nom}}{nV_t}\right) - 1} \tag{16}$$

In addition to that, the currents i_R and i_C of (10) are defined as

$$i_R = \frac{v_p}{\dfrac{N_s}{N_p} r_p}, \tag{17}$$

$$i_C = \frac{N_p}{N_s} c_v \frac{\mathrm{d}v_p}{\mathrm{d}t}, \tag{18}$$

respectively. For simplicity, N_p and N_s escalation terms are assumed as implicit, thus (13), (17) and (18) are reduced to

$$I_D = I_0 \left(\exp\left(\frac{v_p}{N_s n V_t} \right) - 1 \right), \tag{19}$$

$$i_R = \frac{v_p}{R_p}, \tag{20}$$

$$i_C = C_v \frac{\mathrm{d}v_p}{\mathrm{d}t}. \tag{21}$$

We introduce now the state variable q_p in terms of the voltage input v_p and the equivalents circuit's capacitance C_v as

$$q_p = C_v v_p \tag{22}$$

which dynamics is obtained by substituting (17) and (18) in (10). We then obtain

$$\dot{q}_p = -\frac{1}{R_p C_v} q_p + i_s - S i_L. \tag{23}$$

The dynamics of the second state variable ϕ_p is also given by

$$\dot{\phi}_p = \frac{q_p}{C_v}, \tag{24}$$

and since no magnetic storage component is connected to the circuit, then the Hamiltonian function $H_p(q_p, \phi_p)$ of the PV cell farm stage is given by

$$H_p(q_p, \phi_p) = \frac{1}{2C_v} q_p^2 \tag{25}$$

Now, based on the dynamics (23), and (24), together with the Hamiltonian function (25), then PH formulation of a PV cell farm is given by

$$\begin{bmatrix} \dot{q}_p \\ \dot{\phi}_p \end{bmatrix} = \begin{bmatrix} \dfrac{-1}{R_p} & -1 \\ 1 & 0 \end{bmatrix} \begin{bmatrix} \dfrac{\partial H_p}{\partial q_p} \\ \dfrac{\partial H_p}{\partial \phi_p} \end{bmatrix} + \begin{bmatrix} 1 \\ 0 \end{bmatrix} i_s + \begin{bmatrix} -S \\ 0 \end{bmatrix} i_L \tag{26}$$

$$y = \begin{bmatrix}1 & 0\end{bmatrix} \begin{bmatrix} \dfrac{\partial H_p}{\partial q_p} \\ \\ \dfrac{\partial H_p}{\partial \phi_p} \end{bmatrix} = \frac{1}{C_v} q_p = v_p \tag{27}$$

where clearly the input-output port-pair is $(u, y) = (i_s, v_p)$, and (9) holds for (27) since $R_p \geq 0$.

In the next subsections, we introduce the PH formulation of the dc/dc buck converter, the electromechanical stage, and hydraulic system.

B. DC/DC Buck Converter Model

The solar-powered pumped-hydro system requires a dc/dc buck converter in order to reduce the output voltage v_p of the PV farm cell at the input voltage level of the hydro-pump dc motor. The equivalent circuit of the converter is shown in Figure 4 and it is based on the results of [18].

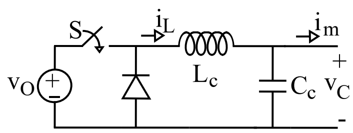

Fig. 4. DC/DC buck converter equivalent electric circuit.

Given a discrete switch S representing a time dependant function that describes the activation and deactivation of input voltage of the equivalent circuit in Figure 4, and the state variables (q_c, ϕ_L) being the charge of the capacitor C_c, and the flux in the inductor L_c, and based on the dynamics

$$L_c \dot{i}_L = -v_C - S R_p i_L + S v_{ph} \tag{28}$$

together with the Biot-Savart Law

$$\phi_L = L_c i_L, \tag{29}$$

and given the Hamiltonian H_c function of the converter

$$H_c(q_c, \phi_L) = \frac{1}{2C_c} q_c^2 + \frac{1}{2L_c} \phi_L^2 \tag{30}$$

then, the dynamics of dc/dc buck converter in Figure 4 is written in the PH formulation such that

$$\begin{bmatrix} \dot{q_c} \\ \\ \dot{\phi_L} \end{bmatrix} = \begin{bmatrix} 0 & 1 \\ \\ -1 & -SR_p \end{bmatrix} \begin{bmatrix} \dfrac{\partial H_c}{\partial q_c} \\ \\ \dfrac{\partial H_c}{\partial \phi_L} \end{bmatrix} + \begin{bmatrix} 0 \\ \\ S \end{bmatrix} v_p + \begin{bmatrix} -1 \\ \\ 0 \end{bmatrix} i_m \tag{31}$$

$$y = \begin{bmatrix}0 & S\end{bmatrix} \begin{bmatrix} \dfrac{\partial H_c}{\partial q_c} \\ \\ \dfrac{\partial H_c}{\partial \phi_L} \end{bmatrix} = S i_L \tag{32}$$

with a chosen input-output port-pair $(u, y) = (v_p, S i_L)$.

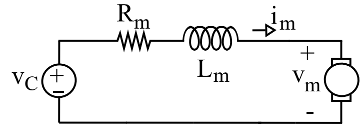

Fig. 5. Pump equivalent circuit.

C. Pump Electrical-Mechanical Model

A pump to storage water from the lower to the upper reservoir is describe in two physic domains. Firstly, the equivalent circuit for the electrical domain is shown in Figure 5. The inductance L_m stores kinetic energy and the dynamic of the system in Figure 5 is described as

$$L_m \dot{i}_m = -R_m i_m + v_C - v_m \tag{33}$$

Also, according to Biot-Savart Law, it can be expressed the magnetic flux ϕ_m as

$$\phi_m = L_m i_m \tag{34}$$

The dynamics of the system allows to include a term q_m related to charge storage in the circuit

$$\dot{q}_m = \frac{\phi_m}{L_m} \tag{35}$$

Since non electric field storage component is connected to the circuit, then the Hamiltonian function is given by

$$H_L(\phi_m, q_m) = \frac{1}{2L_m} \phi_m^2. \tag{36}$$

Thus, from (33), (35) and (36), we define now the dynamic of the pump equivalent electric circuit in terms of the PH framework such that

$$\begin{bmatrix} \dot{\phi_m} \\ \\ \dot{q_m} \end{bmatrix} = \begin{bmatrix} -R_m & -1 \\ \\ 1 & 0 \end{bmatrix} \begin{bmatrix} \dfrac{\partial H_L}{\partial \phi_m} \\ \\ \dfrac{\partial H_L}{\partial q_m} \end{bmatrix} + \begin{bmatrix} 1 \\ \\ 0 \end{bmatrix} v_C + \begin{bmatrix} -1 \\ \\ 0 \end{bmatrix} v_m \tag{37}$$

$$y = \begin{bmatrix} 1 & 0 \end{bmatrix} \begin{bmatrix} \dfrac{\partial H_L}{\partial \phi_m} \\ \\ \dfrac{\partial H_L}{\partial q_m} \end{bmatrix} = i_m, \tag{38}$$

with a chosen input-output port-pair $(u, y) = (v_C, S i_m)$.

Now that the first electrical stage is defined, we elaborate further the dynamics of the mechanical subsection. First, a free body diagram for the equivalent subsection of the pump is shown in Figure 6, which system is described as

$$J_m \dot{\Omega}_m = -B_m \Omega_m + T_m - T_j \tag{39}$$

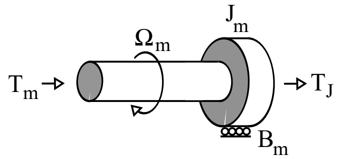

Fig. 6. Pump Mechanical Diagram.

In order to couple the mechanical state to the hydraulic domain, it is required to consider a constant K_h given by

$$K_h = \frac{\Omega_m}{Q_h} = \frac{P_h}{T_J}, \tag{40}$$

where K_h has units of rad/m^3. From the hydraulic system domain shown in Figure 7, we know that

$$P_h = I_h \dot{Q}_h + R_h Q_h + P_{30} + \rho g l \tag{41}$$

and from (41), we rewrite (39) as

$$\beta \dot{\Omega}_m = -\gamma \Omega_m + T_m - \frac{(P_{30} + \rho g l)}{K_h}, \tag{42}$$

with

$$\beta = J_m + \frac{I_h}{K_h^2}, \qquad \gamma = B_m + \frac{R_h}{K_h^2} \tag{43}$$

where β represents an *apparent* mass inertia, and γ includes system's dissipation elements. Based now on the angular displacement Ω_m, we define an angular momentum p_m as

$$p_m = \beta \Omega_m, \tag{44}$$

which in terms of system's dynamics it is convenient to rewrite (44) as

$$\dot{\varphi_m} = \frac{p_m}{\beta} \tag{45}$$

with a Hamiltonian H_m of hydraulic domain system given by

$$H_m(p_m, \varphi_m) = \frac{1}{2\beta} p_m^2. \tag{46}$$

Now, based on (39), (44)-(46), we formulate the dynamics of the mechanical pump stage in the PH framework such that

$$\begin{bmatrix} \dot{p}_m \\ \dot{\varphi_m} \end{bmatrix} = \begin{bmatrix} -\gamma & -1 \\ 1 & 0 \end{bmatrix} \begin{bmatrix} \frac{\partial H_m}{\partial p_m} \\ \frac{\partial H_m}{\partial \varphi_m} \end{bmatrix} + \begin{bmatrix} 1 \\ 0 \end{bmatrix} T_m + \begin{bmatrix} \frac{-1}{K_h} \\ 0 \end{bmatrix} P_{30} + \begin{bmatrix} \frac{-1}{K_h} \\ 0 \end{bmatrix} \rho g l \tag{47}$$

$$y = \begin{bmatrix} 1 & 0 \end{bmatrix} \begin{bmatrix} \frac{\partial H_m}{\partial p_m} \\ \frac{\partial H_m}{\partial \varphi_m} \end{bmatrix} = \Omega_m. \tag{48}$$

with an input-output port-pair $(u, y) = (T_m, \Omega_m)$, with the transducer equations from electrical to mechanical stage of the pump are described as

$$v_m = K_e \Omega_m, \qquad T_m = K_m i_m. \tag{49}$$

D. Hydraulic Pumping Model

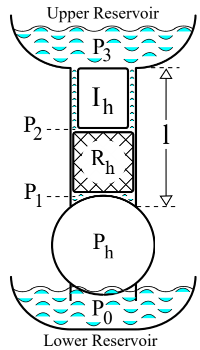

Fig. 7. Hydraulic System Diagram.

The hydraulic pumping system that drives the water from the lower to the upper reservoir is shown in Figure 7. The dynamic of the system can be written as

$$I_h \dot{Q}_h = -R_h Q_h - P_{30} - \rho g l + P_h \tag{50}$$

and based on (39), we can rewrite (50) as

$$\dot{Q}_h = -\left(\frac{R_h + K_h^2 B_m}{\alpha} \right) Q_h - \frac{(P_{30} + \rho g l)}{\alpha} + \frac{K_h}{\alpha} T_m, \tag{51}$$

where α and Γ in (51) are given by

$$\alpha = K_h^2 J_m + I_h \qquad \Gamma = \frac{R_h + K_h^2 B_m}{\alpha^2} \tag{52}$$

being α an apparent mass inertia and Γ having all the dissipative elements of the hydraulic system. Furthermore, it can be considered that the dynamics of the pressure P_{30} in Figure 7 is

$$\dot{P}_{30} = \frac{1}{C_h} Q_h \tag{53}$$

with a Hamiltonian function $H_h(Q_h, P_{30})$ given by

$$H_h(Q_h, P_{30}) = \frac{1}{2} \alpha Q_h^2 + \frac{1}{2} C_h P_{30}^2 + C_h P_{30} \rho g l \tag{54}$$

Finally, based on (51), (53), and (54), we are able to formulate the dynamics of the hydraulic pumping system in the PH framework such that

$$\begin{bmatrix} \dot{Q}_h \\ \dot{P}_{30} \end{bmatrix} = \begin{bmatrix} -\Gamma & \frac{-1}{\alpha C_h} \\ \frac{1}{\alpha C_h} & 0 \end{bmatrix} \begin{bmatrix} \frac{\partial H_h}{\partial Q_h} \\ \frac{\partial H_h}{\partial P_{30}} \end{bmatrix} + \begin{bmatrix} \frac{K_h}{\alpha} \\ 0 \end{bmatrix} T_m \tag{55}$$

$$y = \begin{bmatrix} \frac{K_h}{\alpha} & 0 \end{bmatrix} \begin{bmatrix} \frac{\partial H_h}{\partial Q_h} \\ \frac{\partial H_h}{\partial P_{30}} \end{bmatrix} = K_h Q_h = \Omega_m \tag{56}$$

with an input-output port-pair $(u, y) = (T_m, \Omega_m)$.

IV. SIMULATION RESULTS

For simulation purposes, we have made use of the parameters shown in Table I. The system is adjusted at $24V$ dc-dc converter output voltage when the sun radiation G is $1000W/m^2$, in order to couple the DC Pump [13]. Furthermore, it is necessary to connect an array of 5 PV cells [11] where each one to supplies $175W$. Also, the area per PV Cell is assumed $1.5m^2$ such that the total power from the sun radiated over the PV Cell array reaches $7.5kW$.

Figure 8.a shows that the output energy of the cell under the aforementioned conditions reaches around $875J$. Thus, the efficiency of the PV cell array is around 11.7%. Furthermore, at the output of the hydraulic stage of the system, the shifted mass of water from lower to the upper reservoir is moved by an applied constant energy of $158J$, which results in a total system's efficiency 2.1%. Under this efficiency conditions it is possible to pile up $9.5x10^3J$ of potential energy a minute in the reservoir as shown in Figure 8.b. The accumulated potential energy represents a volume of water of $0.09m^3/min$ as shown in Figure 8.c, or a equivalence of $5.4m^3/h$. This result is consistent with the specifications of the pump under test, whose maximum specified flow rate is is $6.5m^3/h$.

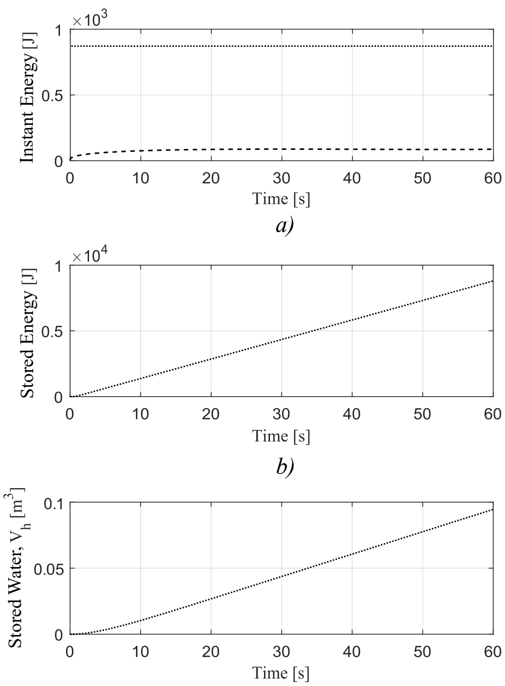

Fig. 8. a) PV cell output energy (solid line) and energy applied to shift of water at the upper reservoir (dashed line); b) potential recovered energy stored at the upper reservoir; c) volume of recovered water at the upper reservoir.

V. CONCLUDING REMARKS

A model of a solar-powered pumped-hydro system to recover potential energy from the water is successfully modelled and simulated, under ideal conditions of constant solar radiation. We have assumed that the system feeds a dc pump in an open loop system. An energy-based approached is here chosen based on the port-Hamiltonian framework in order to model the multi-system domain. According to simulation results, the system efficiency could be enhanced by replacing the actuators and/or elements (motor, pumps, cells, pipes) to other ones with more appropriate specifications. Further modifications of the model are required to add a power control in order to simulate the behaviour of the system to a variable power input.

REFERENCES

[1] R. Brackett, "For 300 Days, Costa Rica Generated Electricity from Renewable Sources Alone," United States, 2018. [Online]. Available: https://weather.com/news/news/2018-12-21-costa-rica-300-days-energy-renewable-sources

[2] C. Marshall, "Costa Rica bids to go carbon neutral," United Kingdom, 2008.

[3] J. Wright, "Estudio del potencial solar en Costa Rica," *Uniciencia*, vol. 23, no. 1-2, pp. 19–40, 2009.

[4] T. Ma, H. Yang, L. Lu, and J. Peng, "Technical feasibility study on a standalone hybrid solar-wind system with pumped hydro storage for a remote island in Hong Kong," *Renewable energy*, vol. 69, pp. 7–15, 2014.

[5] C. Bueno and J. A. Carta, "Wind powered pumped hydro storage systems, a means of increasing the penetration of renewable energy in the Canary Islands," *Renewable and sustainable energy reviews*, vol. 10, no. 4, pp. 312–340, 2006.

[6] O. Paish, "Small hydro power: technology and current status," *Renewable and sustainable energy reviews*, vol. 6, no. 6, pp. 537–556, 2002.

[7] A. van der Schaft, *L_2-Gain and Passivity Techniques in Nonlinear Control*. London, UK: Springer, 2000.

[8] A. van der Schaft and D. Jeltsema, *Port-Hamiltonian systems theory: An introductory overview*. Now Publishers Inc., 2014, vol. 1, no. 2-3.

[9] V. Duindam, A. Macchelli, S. Stramigioli, and H. Bruyninckx, *Modeling and Control of Complex Physical Systems: The Port-Hamiltonian Approach*. Berlin, Germany: Springer, 2009.

[10] J. Johnson, D. Schoenwald, S. Kuszmaul, J. Strauch, and W. Bower, "Creating dynamic equivalent pv circuit models with impedance spectroscopy for arc fault modeling," in *2011 37th IEEE Photovoltaic Specialists Conference*. IEEE, 2011, pp. 002 328–002 333.

[11] S. V. LIMITED, "SURANA SVL-175 Polycrystalline PV Module Datasheet," Secunderabad, India. [Online]. Available: http://suranasolar.com/175w.pdf

[12] KAG DC, "Motors Catalogue 2015/2016," Hannover, Germany, 2016. [Online]. Available: https://www.kag-hannover.com/wp-content/uploads/dokumente/Katalog/EN/KAG-DC_Motors-Catalogue_2015_2016.pdf

[13] Marsrock, "Water Pump Model RD9024 Datasheet," Fujian, China. [Online]. Available: https://www.amazon.com/MarsRock-Clean-Water-Outlet-Approved/dp/B076BJXKB1

[14] L. D. Murillo-Soto, G. Figueroa-Mata, and C. Meza, "Identification of the Internal Resistance in Solar Modules Under Dark Conditions Using Differential Evolution Algorithm," in *2018 IEEE International Work Conference on Bioinspired Intelligence (IWOBI)*. IEEE, 2018, pp. 1–9.

[15] C. Meza, V. Virtuani, and D. Chianese, "Evaluation of models for the internal capacitance of a pvmodule for the design and simulation of power converters," in *25th European Photovoltaic Solar Energy Conference and Exhibition*, 2010.

[16] Y. Chaibi, M. Salhi, A. El-jouni, and A. Essadki, "A new method to extract the equivalent circuit parameters of a photovoltaic panel," *Solar Energy*, vol. 163, pp. 376–386, 2018.

[17] M. G. Villalva, J. R. Gazoli, and E. Ruppert Filho, "Comprehensive approach to modeling and simulation of photovoltaic arrays," *IEEE Transactions on power electronics*, vol. 24, no. 5, pp. 1198–1208, 2009.

[18] B. Wang, V. R. K. Kanamarlapudi, L. Xian, X. Peng, K. T. Tan, and P. L. So, "Model predictive voltage control for single-inductor multiple-output DCDC converter with reduced cross regulation," *IEEE Transactions on Industrial Electronics*, vol. 63, no. 7, pp. 4187–4197, 2016.